

Regular paper

Modeling and Control of Switched Reluctance Motor for Automotive Applications

Mohamed YAICH¹, Mohamed Radhouan HACHICHA², Moez GHARIANI¹ and Rafik NEJI²

¹.Lab –ESSE,².Lab-LETI : University of Sfax, National School of Engineers-Tunisia. E-mail :yaich_fr2000@yahoo.fr



Journal of Automation
& Systems Engineering

Abstract-Switched reluctance machines, because of their simple construction and low manufacturing cost are gaining importance in consideration for automotive applications. Recently, SRMs have been considered for use as a propulsion motor in electric and hybrid vehicle applications. The major limitations of the switched reluctance machine technology are its acoustic noise and high torque ripple as compared to other types of electric machines. Recently, two primary approaches to reduce the torque pulsations were essentially developed. One method is to improve the magnetic design of the motor, while the other is to use sophisticated electronic control techniques. In this work, modeling, simulation and analysis of Switched Reluctance motor has been done. Two control loops- conventional PI controller based speed loop and conventional hysteresis controller current loop- have been used. The whole work is done in Matlab/Simulink environment.

Keywords: Switched reluctance motor, PI Control, hysteresis band current controller, Hybrid Vehicle.

1. INTRODUCTION

The power electronic converters and electric propulsion motors are crucial components for modern hybrid electric vehicle (HEV). Accordingly, it is necessary that the associated traction motor and drive, operate at their optimal effectiveness throughout the test cycle. In typical HEV propulsion the electric motor is used over the entire operating range of torque / speed. SRMs are beginning to gain interest as a potential candidate for HEV propulsion due to their simple and rugged construction, fault tolerant operation, insensitivity to high temperatures, an extremely long constant-power range and high speed operation [1-2]. In this motor only the stator has got windings. The rotor contains no conductors or permanent magnets [3]. It consists simply of steel laminations stacked onto a shaft. It is because of this simple mechanical construction SRMs carry the promise of low cost, which in turn has motivated a large amount of research on SRMs in the last decade. Due to its non-linear nature, the switched reluctance motor has an intrinsic ripple torque oscillation in the rotor axis. There are many strategies and methods to reduce ripple torque in this type of machine. Essentially, we can present two initial approaches for the reduction of the oscillation: the first consists on improving the magnetic design of the machine, and another is based on the use of electronic control. Several analytic methods for SRM design have been presented [4-5]. The designers of electrical machines take into consideration, The designers of electrical machines take into consideration its non-linear magnetic characteristics. Project the structure of the polar regions of the stator and the rotor, so that the machine can operate in stabilized speed, without torque oscillation. Many articles have been written in this field. however, These strategies excessively limit the speed band operation of the SR Motor [6].

The SRM geometry can be optimized by modifying stator and rotor's diameters or there pole shapes. Moreover the number of phases can be reduced in such cases as in [7].The other study, concentrated in the converter design and in the control strategy, is based on selecting the best combination of parameters operation which include voltage, energization and desenergization angles, and current profile. There are countless proposals for torque oscillation reduction using diverse types of control and modeling. In this paper the technical control for reduction of ripple based in a Hysteresis current controller and propotional integrator speed controller .

2. SRM CHARACTERISTICS

The basic operating principle of the SRM is quite simple; as current is passed through one of the stator windings, torque is generated by the tendency of the rotor to align with the excited stator pole. The direction of torque generated is a function of the rotor position with respect to the energized phase, and is independent of the direction of current flow through the phase winding. Continuous torque can be produced by intelligently synchronizing each phase's excitation with the rotor position. The basic 3-phase SRM structure has 6 stator and 4 rotor poles . Each stator and rotor pole has pole arc of 30° mechanical. The stator windings on diametrically opposite poles are connected either in series or in parallel to form one phase of the motor. When a stator phase is energized, the most adjacent rotor pole-pair is attracted toward the energized stator to minimize the reluctance of the magnetic path. Therefore, by energizing consecutive phases in succession, the SRM develops reluctance torque in either direction of rotation. Fig.1 shows its linear inductance profile $L(\theta)$ with each phase inductance displaced by an angle θ_s given by inductance profile of each phase .

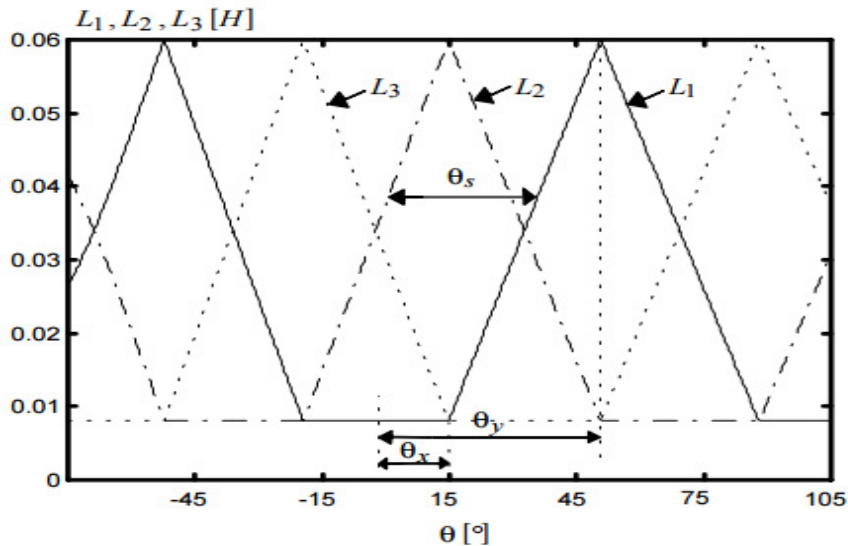


Figure 1 SRM linear model. Inductance profile of each phase

$$\theta_s = 2\pi \left(\frac{1}{N_r} - \frac{1}{N_s} \right) \quad (1)$$

Where N_r and N_s are the number of rotor and stator poles, respectively. When the motor has equal rotor and stator pole arcs, $\beta_r = \beta_s$, we get the following angle relations:

$$\theta_x = \left(\frac{\pi}{N_r} - \beta_r \right) \quad (2)$$

$$\theta_y = \frac{\pi}{N_r} \quad (3)$$

Fig. 2 shows the angle δ corresponding to the displacement of a phase in relation to another, which is given by

$$\delta = 2\pi \left(\frac{1}{N_r} - \frac{1}{N_s} \right) \quad (4)$$

The studied 6/4 SRM has the following parameters:

$L_{min} = 8$ mH, $L_{max} = 60$ mH, and $\beta_r = \beta_s = 30^\circ$. Thus, from (2) and (3), we get $\theta_x = 15^\circ$ and $\theta_y = 45^\circ$.

The electric equation of each phase is given by:

$$\frac{\partial \psi_{i(\theta, I_i)}}{\partial t} + RI_i = V \quad (5)$$

With $i = \{1, 2, 3\}$

While excluding saturation and mutual inductance effects, the flux in each phase is given by the following linear equation:

$$\psi_{i(\theta, I_i)} = L(\theta) I_i \quad (6)$$

The total energy associated with the three phases ($n = 3$) is given by:

$$W_{total} = \frac{1}{2} \sum_{i=1}^3 L(\theta + (n-i-1)\theta_s) I_i^2 \quad (7)$$

and the motor total torque by:

$$\Gamma = \frac{1}{2} \sum_{i=1}^3 \frac{\partial L(\theta + (n-i-1)\theta_s)}{\partial \theta} I_i^2 \quad (8)$$

The mechanical equations are:

$$J \frac{\partial \omega}{\partial t} = \Gamma - \Gamma_l - f \omega \quad (9)$$

Where Γ_l represents the torque load, and f the machine friction coefficient. The angular velocity can be written as follows :

$$\frac{\partial \theta}{\partial t} = \omega \quad (10)$$

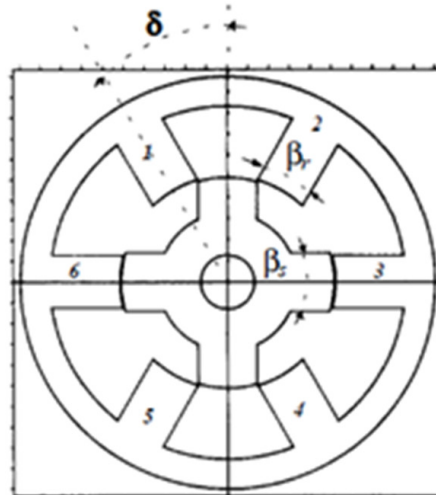


Figure 2 The angle δ corresponding to displacement of a phase in relation to another

We show in Fig. 3 the simulation diagram used for the SRM simulation using Simulink, which is the use of conventional blocks allowing understanding the programmed structure more easily.

Fig. 4 shows the content of the block phase 1. It contains four other blocks, each one associated with a specific Matlab function. The complete model can be used in application of Hybrid Electric Vehicle with proper turning on/off of the operating mode region of SRM/Gs.

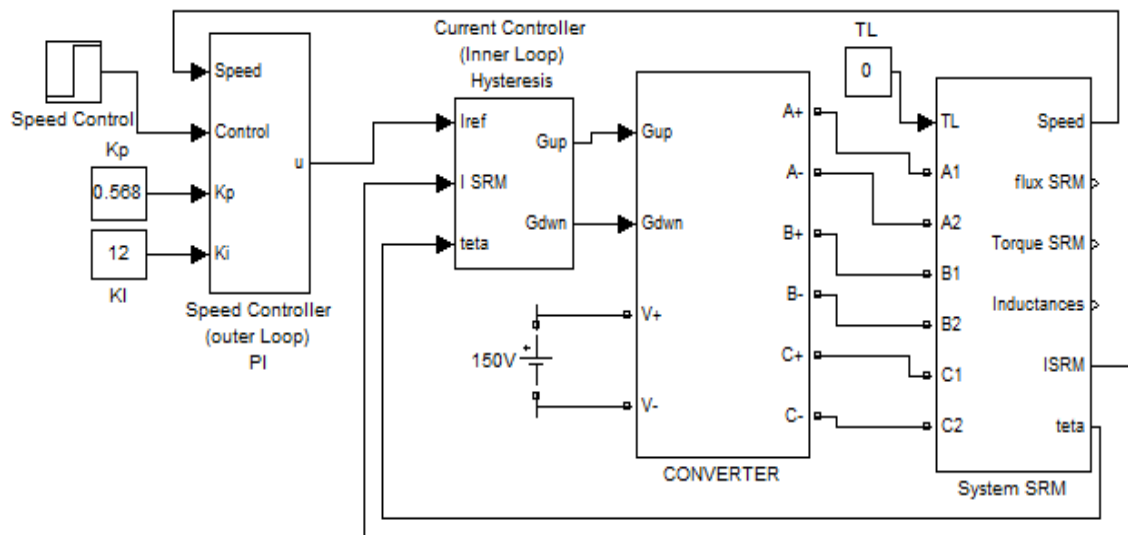


Figure 3 Matlab/Simulink diagram of SRM linear model

does not depend on the current sign but only on $\frac{\partial L}{\partial \theta}$ sign.

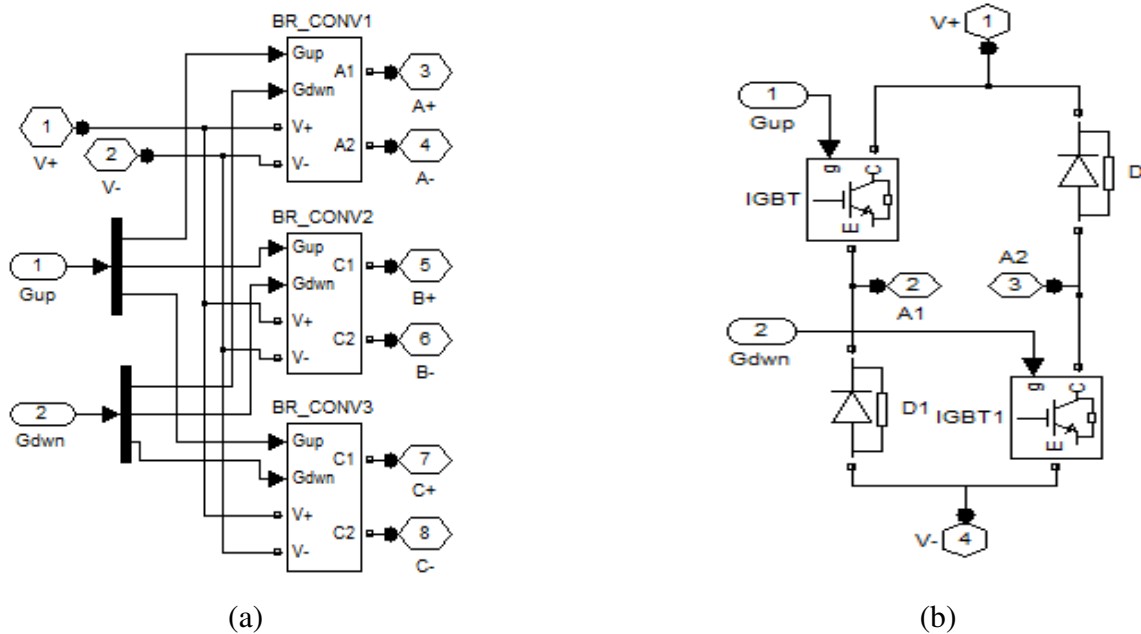


Figure 5 H-bridge asymmetric converter: (a) Power converter detail, (b) Phase detail

4. SRM CONTROLLEUR STRATEGIES

The effective performance characteristics from a SRM drive system can be obtained by proper positioning of the phase excitation pulses relative to the rotor position. The commutation angles (turn-on angle θ_{on} , turn-off angle θ_{off}), total conduction period and the magnitude of the phase current (I_{ref}) determine the average torque, torque ripple and other performance parameters. The difficulty to find the control parameters depends on the chosen control method for a particular application. At low speeds, the current rises almost instantaneously after turn-on because of the negligible back-emf and the current must be limited by either controlling the average voltage or by regulating the current level. As the speed increases, the back-emf increases and opposes the applied bus voltage. Phase advancing is necessary to establish the phase current at the onset of rotor and stator pole overlap region. Voltage PWM or chopping control is used to force maximum current into the motor to maintain the desired torque level. The torque command is executed by regulating the current in the inner loop as shown in the closed-loop block diagram in Figure 6. The desired current " I_{ref} ", is dependent upon the load characteristics, speed and control strategy. The simpler control strategy is to generate one current command to be used by all the phases in succession. The electronic switch selects the appropriate phase for current regulation based on θ_{on} , θ_{off} and the instantaneous rotor position. The current controller generates the gating signal for the power devices based on the information coming from the electronic switch. With both the switches turned ON, the energizing current in the phase winding increases with positive DC-link voltage. For current control, the switches are operated to freewheel, magnetize and demagnetize depending on the rotor position and direction. The current in the switched phase is quickly brought to zero applying "-Vdc", while the incoming phase ensures the torque production depending on the used current. The torque ripple tends to increase since the torque production is not smooth during phase

transition in these drives. Usually, three kinds of current controllers are used for the SRM, namely: PI controller, hysteresis controller and hybrid structure which is a combination of the first two.

In this project, the hysteresis current controller is used for its simplicity [12]. There are many choices for the outer speed controller, such as PID controller, two degree of freedom controller, fuzzy controller, adaptive controller, and artificial neural network controller. The standard proportional-integral (PI) controller is used in this research for simplicity.

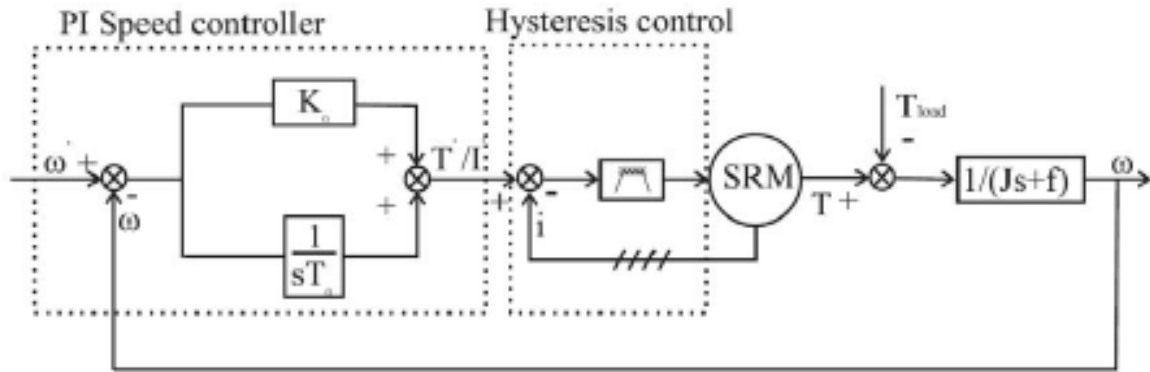


Figure 6 Closed-loop speed and current control block diagram of a SRM [11]

4.1 Closed loop current controller design

Current feedback is essential for this proposed control strategy. Here each of the phase-currents are sensed and fed back to controller. A hysteresis controller (soft chopping) is used to control the phase current according to reference current generated by the speed controller. Therefore, soft switching is often preferred for motoring operation [13]. Here the only control parameter is the hysteresis band Δi . In the case of an analog implementation, this parameter ensures that the instantaneous current is bounded between $i^* \pm \Delta i/2$, where i^* is the desired current. In this case, the current ripple is equal to Δi and the current controller output takes only two distinct values $+V_{dc}$ and zero. It generates switching pulses by comparing reference current and sensed current as mentioned below:

If, $i_{act} < I_{Lw}$, switch is turned on.
and $i_{act} > I_{Up}$, switch is turned off.

4.2 Speed control loop

In this paper, the design of a speed controller for the switched reluctance motor using proportional-Integral control strategy is presented. While Proportional-Integral control represents one of the simplest strategy, its implementation for driving an SRM has not been extensively investigated before, and its good performance is apparent. In the competition with more advanced controllers. The P-I controller has generally been regarded as the one most likely to succeed in industrial applications. The main reasons for this have been simplicity, lower cost, zero steady-state error, ease of implementation, robustness, good speed of response, good stability, and other desirable features. P-I controllers are extensively used in many drives where speed control is desired. A P-I control law is chosen only because of the above-mentioned reasons and is not intended to infer that this is the best control law.

Our control objective is to track a reference speed trajectory. Each phase is provided with current during the torque productive period of rotation, and the amplitude of the current is adjusted such that the desired level of torque is obtained. This desired level is dictated by an external feedback loop for controlling the speed.

The PI controller parameters calculated according a small- signal model of the SRM drive system, to satisfy the control specification. The transfer function of the PI speed controller and the open-loop gain of the speed control loop are given by Eqs.(14) and (15), respectively. Current loop gain taken as unity [14-16].

$$G_{(s)} = \frac{K_s(1 + ST_s)}{ST_s} \quad (14)$$

$$G_s^0(s) = \frac{K_s(1 + ST_s)}{ST_s} \cdot K_T \cdot \frac{1}{F + JS} \quad (15)$$

Where, K_T is the torque constant. In order to obtain correct simulation results, knowing the accurate values of J and F is crucial.

5. SIMULATIONS RESULTS

SRM system is simulated using MATLAB/Simulink software. The parameters of the motor used for simulation studies are given in appendix.

The firing angles: turn-on and turn-off are kept fixed throughout the simulation studies at 0 deg and 30 deg (where 0deg and 90 deg correspond to aligned and unaligned positions). Only one phase is allowed to be excited at one time.

The SRM is fed in this simulation using the asymmetrical power converter in which, each leg consists of two IGBTs and two freewheeling diodes. Thus, the phase currents are independently controlled by an hysteresis current controller which engender the IGBTs drive signals by comparing the measured currents with the references. The IGBTs switching frequency is determined using the hysteresis band for a previous optimal study fixed at $\Delta I = \pm 0.1A$. a PI classic controller is used to regulate the speed values of proportional constant $K_p=0.568$ and integral constant $K_i=12$ fixed yet.

With the motor functioning without load, waveforms can be obtained by integrating all the functional blocks in the motoring simulation figure 3 such as position wrapping, active phase determination, phase commutation and current regulation. Figure 7 shows inductance variation in SRM, which is considered as control reference for the phase commutation, it starts from 0.008 H, then it increases to 0.06 H, and falling back to 0.008 H. The speed response is depicted in Figure 8, when the motor is commanded to accelerate from rest to 100 rad/s without load. It can be seen from the figure that the motor speed converges to the desired speed. It should be mentioned that the ripple in the speed response is due to the sequential switching between the phases and it is not caused by controller [17]. Figure 9 shows the total torque variation in time of all the three phases, the total electromagnetic torque is about 4 Nm. Torque ripple presents high magnitude for the used values of Turn-on (θ_{on}) and Turn-off (θ_{off}) angles, having as consequence to originate important speed oscillations shown in figure 8. To decrease the speed oscillations it is necessary to produce more torque. Adjustment of the Turn-off angle value allowed fewer oscillations. However, ripple reduction is not an easy task because other parameters, such as the speed and load values, influence the torque ripple magnitude. Figure 10 gives the flux-linkage and gate signal of the converter phase PWM switching voltages for regulating the current in time. Here, the ripples are due to the current chopping control [18]. The phase current is given in

figure 11. It can be seen that the current flows only in the inductance rising slope as it is in motoring mode, also the phase current regulation between the turn-on and turn-off positions for motoring operation.

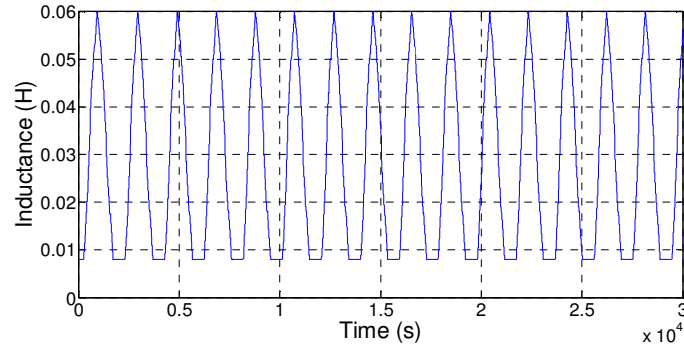


Figure 7 Inductance profile

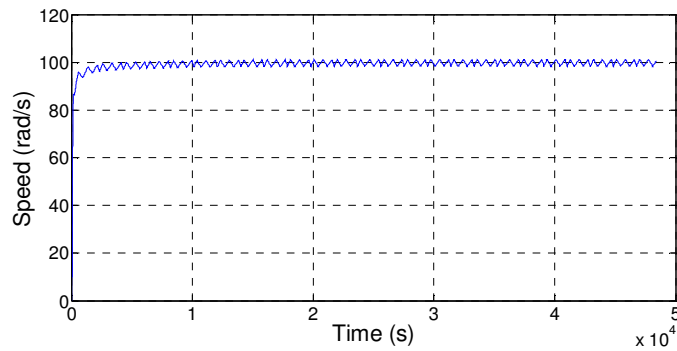


Figure 8 Speed Characteristics

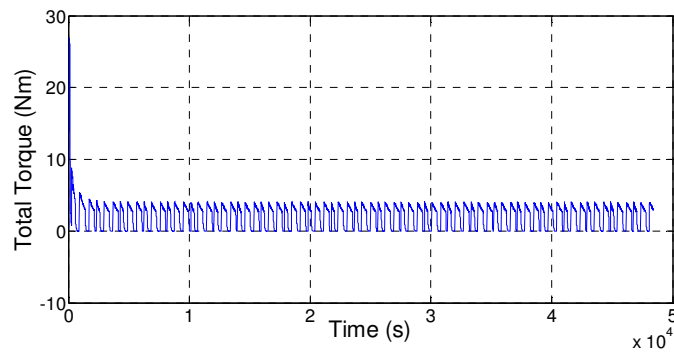


Figure 9 Total torque

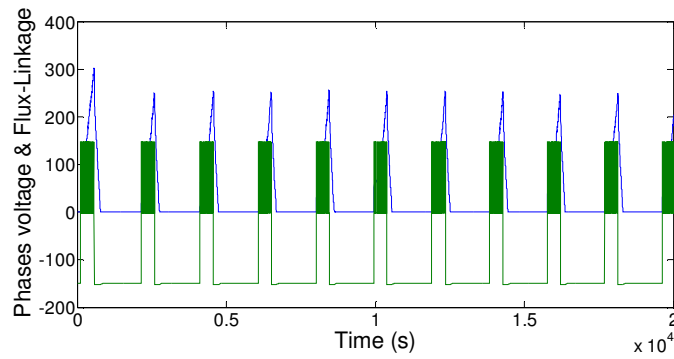


Figure 10 Phase Voltage and Flux-Linkage

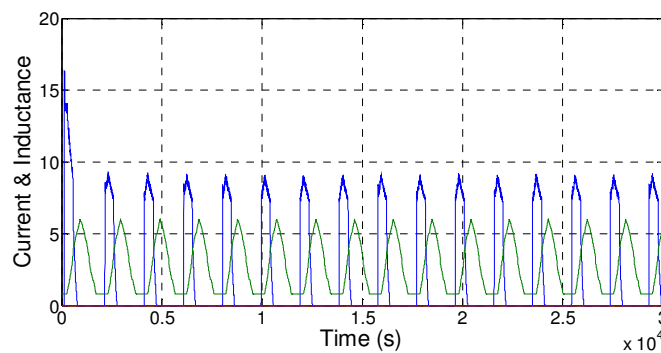


Figure 11 Current and Inductance

6. CONCLUSIONS

This paper presents a new SRM simulation model, 3-phase 6-stator pole and 4-rotor pole which will be applied for the small hybrid electric vehicle (HEV). This model has three independent modules; the controller module, the power converter module and SRM module. With a focus on the motor and its controller design. This enables it to be used in other types of reluctance motor and for different control strategies in automotive applications. We presented a description of the system and developed the mathematical formulation, the numerical method for simulation and gave a detailed discussion on the constraints, boundary conditions and approximations considered by the simulation work. To accurately analyze torque oscillations, we checked several simulations in order to reliably identify the SRM dynamic behavior. We mainly focused on the influence of the choice of the angle Θ_{off} on the dynamic behavior.

This work investigates the application of traditional PI for speed controller and technique of hysteresis for current controller, to control the highly non-linear variable reluctance motors. The dynamic behaviors of the drive system with this control were presented and discussed. This control scheme guarantees that the speed asymptotically converges to the desired speed.

Appendix

Parameters of the system used in simulation:

Phase number 3.

Number of stator poles 6; 30° pole arc.

Number of rotor pole 4; pole arc 30°.

Maximum inductance 60 mH (unsaturated); Minimum inductance 8mH;
Phase resistance $R=1.30\Omega$; Moment of inertia $J=0.0013 \text{ Kg/m}^2$; Friction $F=0.0183 \text{ Nm/s}$;
Inverter Voltage $V=150 \text{ v}$.

REFERENCES

- [1] M.Krishnamurthy, C.S.Edrington, A.Emadi, P.Asadi, M.Ehsani, and B.Fahimi, "Making the case for applications of switched reluctance motor technology in automotive products," *IEEE Trans. on Power Electronics*, vol.21, pp. 659-675, May 2006.
- [2] S. Wang, Q. Zhan, Z. Ma, and L. Zhou, "Implementation of a 50-kW four-phase switched reluctance motor drive system for hybrid electric vehicle," *IEEE Trans. on Magnetics*, vol. 41, part 2, pp. 501-504, Jan. 2005.
- [3] Adrian David Cheok et al, (2002), "A New Torque and Flux Control Method for Switched Reluctance Motor Drives", *IEEE Transaction on Power Electronics*. Vol.17, No.4, pp. 543-557.
- [4] A. Radun, "Analytical calculation of the switched reluctance motor's unaligned inductance", *IEEE Trans. on Magn.*, Vol.35, no.6, Nov. 1999.
- [5] D.N. Essah and S.D. Sudhoff, "An improved analytical model for the switched reluctance motor", *IEEE Transactions on Energy Con* , Vol.33, no.6, Nov. 1997.
- [6] Sihem Saidani, Moez Ghariani, "Dynamic behavior of 12/8 switched reluctance motor" *Sciences and Techniques of Automatic Control and Computer Engineering (STA)*, 2015 16th International Conference.
- [7] R. T. Naayagi and V. Kamaraj, "Optimum Pole Arcs for Switched Reluctance Machine with Reduced Ripple," in *2005 International Conference on Power Electronics and Drives Systems*, vol. 1, pp. 761–764.
- [8] Jayanta Mukhopadhyay , Sumana Choudhuri, Samarjit Sengupta, "drive strategies for switched reluctance motor – a review" *Michael Faraday IET International Summit 2015* ; doi: 10.1049/cp.2015.1619.
- [9] J. G. Amoros ; B. B. Molina ; P. A. Gascon, "Simulation of linear switched reluctance motor drives". *IEEE Power Electronics and Applications (EPE 2011)*, Proceedings of the 2011-14th European Conference.
- [10] Samia M. Mahmoud, Mohsen Z. El-Sherif, and Emad S. Abdel-Aliem, "Studying Different Types of Power Converters Fed Switched Reluctance Motor," *International Journal of Electronics and Electrical Engineering* Vol. 1, No. 4, December, 2013-doi: 10.12720/ijeee.1.4.281-290
- [11] Sihem Saidani, Moez Ghariani. "Static Simulation of a 12/8 Switched Reluctance Machine (Application: Starter-Generator)", *Intelligent Control and Automation*, 2015, 271-288. Published Online November 2015 in SciRes. <http://www.scirp.org/journal/ica> <http://dx.doi.org/10.4236/ica.2015.64025>
- [12] Mohseni, Mansour and Islam, Syed M. and Masoum, Mohammed A.S. 2011. Enhanced Hysteresis-Based Current Regulators in Vector Control of DFIG Wind Turbines. *IEEE Transactions on Power Electronics*. 26 (1): pp. 223-234.

- [13] Maged N. F. Nashed, Samia M. Mahmoud, Mohsen Z. El-Sherif, Emad S. Abdel-Aliem., “ Hysteresis Current Control of Switched Reluctance Motor in Aircraft Applications”.IOSR Journal of Engineering (IOSRJEN). ISSN (e): 2250-3021, ISSN (p): 2278-8719. Vol. 04, Issue 03 (March. 2014), ||V5|| PP 25-40
- [14] Jaehyuck Kim, Yong-hoe Jeong, Yong-Hee Jeon, Jun-Ho Kang, Seunghun Lee, and Jang-Yeop Park., “Development of a Switched Reluctance Motor-based Electric AC Compressor Drive for HEV/E Applications”. Journal of Magnetism 19(3), 282-290 (2014).
- [15] R. Krishnan, —Switched Reluctance Motor Drives,|| book by CRC press, Boca Raton, London, New York Washington, D.C.
- [16] Jie Dang ., “Switched Reluctance Machine Electromagnetic Design and Optimization ”, Ph.D. Dissertation, Georgia Institute of Technology .August 2015.
- [17] Muthana T. Alrifai , Mohamed Zribi & Hebertt Sira-Ramirez (2004) Static and dynamic sliding mode control of variable reluctance motors, International Journal of Control, 77:13, 1171-1188, DOI: 10.1080/002071704200024383.
- [18] Yves Mollet, Mathieu Sarrazin, Herman Van der Auweraer, Johan Gyselinck “Experimental Noise and Vibration Analysis of Switched Reluctance Machines – Comparison of Soft and Hard Chopping in Transient Conditions”. in 4th International Conference on Renewable Energy Research and Applications (ICRERA), 2015, pp. 1-8.